PRELIMINARY

WAVE PROPAGATION IN GROOVE GUIDES*

H. Y. Yee and N. F. Audeh, member, IEEE

SUMMARY:

19691

A groove guide consists of two parallel conducting plates with two grooves cut at the center in the longitudinal direction. The air filled deformed guide can be transformed into a parallel-plane guide filled with a nonunifom aniostropic dielectric. The posed boundary value problem was solved by approximation techniques; the results were experimentally verified. The groove guide has the advantages of transporting most of the energy in the groove region, having a very low attenuation constant and, under certain conditions, propagating the dominant modes only.

AUTHOR

* This research work was supported by the National Aeronautics and Space Administration partially funded under NsG-381.

The authors are with the University of Alabama Research Institute, Huntsville, Alabama.

1. INTRODUCTION

A groove guide consists of two parallel conducting planes with two identical grooves facing each other, cut at the center and parallel to the direction of propagation as shown in Fig. 1. The impedance-matching concept, and the transverse resonance method were discussed by Rudy[1], and Nakahara and Kurauchi[2] respectively. Their discussions were restricted to rectangular grooves. Tischer[3] formulated a different approach based on conformal mapping which is more general and thus is applicable to guides with arbitrarily shaped grooves. Non-rectangular grooves are often desirable especially in the consideration of high power problems.

The purpose of this paper is to obtain a solution utilizing the last approach. Approximate techniques will be used to obtain a solution of the wave equation and the characteristics of the guide such as the cut-off frequency, guide wavelength, field distribution, attenuation, and decay constant. Experimental results confirm the theoretical solution quite well.

There are three salient features of groove guides which can be deduced from the approximate solution.

(i) Energy transfer is concentrated in the region of the groove, for the field decays exponentially in the transverse direction.

(ii) The attenuation constant of the groove guide due to the finite conductivity of its walls decreases with frequency, and always less than that of the conventional parallel-plane waveguide made of the same material.

(iii) There are certain conditions for the geometry of grooves such that no higher order modes can propagate.

2. FORMULATION

Let the boundaries of an arbitrarily grooved air-filled waveguide be the coordinate surfaces $u = a$ and $u = -a$ as shown in Fig. 1(a). The orthogonal curvilinear coordinates u, v, and z in the W-space are numerically equal to the cartesian coordinates x, y, and z in the Z-space respectively. The cross section of the parallel-plane guide in the Z-space, as shown in Fig. 1(b), is the transform of the cross section of the groove guide in the W-space. The infinitesimal line element in the orthogonal curvilinear coordinates in the W-space is given as

$$(ds)^2 = [\,h(u,v)\,du\,]^2 + [\,h(u,v)\,dv\,]^2 + (dz)^2$$

where h is the metrical coefficient. In the Z-space the element in Cartesian coordinates is

$$(ds)^2 = (dx)^2 + (dy)^2 + (dz)^2$$

By comparing the scalar components of the Maxwell's equations in these two systems and noting that the permeability and the permittivity in the Z-space are tensors, it is found that the two systems are equivalent if [3,4]

$$\begin{bmatrix} h\,H_u \\ h\,H_v \\ H_z \end{bmatrix} \equiv \begin{bmatrix} H_x \\ H_y \\ H_z \end{bmatrix} \quad , \quad \begin{bmatrix} h\,E_u \\ h\,E_v \\ E_z \end{bmatrix} \equiv \begin{bmatrix} E_x \\ E_y \\ E_z \end{bmatrix} \qquad (1)$$

$$\bar{\mu} = \mu_o\,\bar{\xi} \qquad \text{and} \qquad \bar{\epsilon} = \epsilon_o\,\bar{\xi}$$

where

$$\xi = \begin{bmatrix} 1 & 0 & 0 \\ 0 & 1 & 0 \\ 0 & 0 & h^2 \end{bmatrix}$$

The matrix coefficient h, which is a function of x and y, is given by

$$h^2 = \left(\frac{\partial p}{\partial x}\right)^2 + \left(\frac{\partial q}{\partial x}\right)^2 = \left(\frac{\partial p}{\partial y}\right)^2 + \left(\frac{\partial q}{\partial y}\right)^2 \tag{3}$$

where p and q are cartesian coordinates in the W-space which are functions of u and v, and therefore functions of x and y. Actually Eq. (3) implies that the two coordinate systems are interrelated by conformal transformation, since if

$$R = p(u,v) + jq(u,v)$$

$$Z = x + jy$$

and

$$R = f(Z) \tag{4}$$

then $\left|\frac{dR}{dZ}\right|^2$ is identically equal to h^2 as given by Eq. (3). The quantity h^2 can then be found analytically or graphically by conformal mapping.

It can therefore be concluded that the air-filled groove guide can be transformed by conformal mapping into a parallel-plane waveguide filled with a nonuniform anisotropic material described by Eq. (2).

Let an electromagnetic wave propagate in the z-direction within the parallel-plane guide in the Z-space. All field components have the same z-dependence of the form $\exp(-jk_z z)$ where k_z is the propagation constant. By manipulating Maxwell's equations for wave propagation inside such a guide the resulting wave equation will be

$$\nabla_\perp^2 \psi(x,y) + k^2 h^2(x,y)\, \psi(x,y) = 0 \tag{5}$$

where

$$k^2 = k_o^2 - k_z^2$$

$$k_o^2 = \omega^2 \mu_o \epsilon_o$$

$$k_z = 2\pi/\lambda_y$$

The quantity λ_g is the groove guide wavelength, and $\nabla_\perp^2$ is the transverse Laplacian operator. The wave function $\psi = H_z(x,y)$ for TE modes, and $\psi = E_z(x,y)$ for TM modes. It should be kept in mind that the z-dependence has been removed from the wave function. Whenever suitable solutions of Eq. (5) are found for the pertinent boundary conditions, the transverse components can readily be found by using Maxwell's equations which are reduced to the following form:

$$\overline{E} = (-jk_z/k^2)\,[\,\nabla_\perp E_z + (\omega\mu_o/k_z)\;\nabla_\perp \times (H_z\overline{z})\,] \tag{6a}$$

$$\overline{H} = (jk_z/k^2)\,[\,(\omega\epsilon_o/k_z)\;\nabla_\perp \times (E_z\overline{z}) - \nabla_\perp H_z\,] \tag{6b}$$

where $\overline{z}$ is a unit vector in the z-direction.

The last step in this procedure is to transform the above solution from the Z-space into the W-space. This can easily be done by using the identities in Eq. (1).

3. SOLUTION OF THE WAVE EQUATION

The exact solution of the wave equation for the case of the parallel-plane guide loaded with nonuniform anisotropic dielectric is in general not known. Approximate techniques will be used and experimental results verify the approximate solution.

Let the groove be confined to the central region and symmetrical with respect to the z-axis, [see Fig. 1(a)]. There exists, therefore, a region, $-a \leq x \leq a$, outside of which $h \approx 1$. The loaded parallel-plate guide can now be divided into three sections, as shown in Fig. 2. In regions I and III, where $x \geq a$, and $h \approx 1$, the guide is uniformly filled. In region II, however, where $-a \leq x \leq a$, the guide is filled with a hypothetical medium as described by Eq. (2).

Under these assumptions, the solutions to the guided waves will be handled separately according to their classifications, TE or TM modes.

a. TE Modes:

The wave function in the wave equation (5) represents H_z in the TE modes. The boundary conditions are:

(i) At $x = +a$

$$\psi^{I} = \psi^{II} \quad \text{and} \quad \frac{\partial \psi^{I}}{\partial x} = \frac{\partial \psi^{II}}{\partial x} \tag{7}$$

(ii) At $x = -a$

$$\psi^{III} = \psi^{II} \quad \text{and} \quad \frac{\partial \psi^{III}}{\partial x} = \frac{\partial \psi^{II}}{\partial x} \tag{8}$$

(iii) At $y = 0,\ b$

$$\frac{\partial \psi}{\partial y} = 0 \tag{9}$$

where b is the width of the guide and ψ without superscript is valid for any of the three regions.

Under the above conditions, let it be assumed that the even solution of the wave equation for the TE_{mn} mode is of the following form:

$$\psi_e^{I,III} = \sum_{p,q} A_{pq}\, e^{\mp \alpha_{pq} x} \cos \frac{q\pi y}{b} \tag{10}$$

$$\psi_e^{II} = \sum_{p,q} C_{pq} \cos \beta_{pq} x \cos \frac{q\pi y}{b} \tag{11}$$

where the subscript "e" stands for the even solutions, and the summations are taken over all possible integers. The quantities α_{pq} and β_{pq} are constants yet to be determined. The odd solutions will be considered later.

If Eq. (10) is substituted in Eq. (5), and the value of h is taken as unity, then for $x \geq a$ the wave equation becomes:

$$\sum_{p,q} [\alpha^2_{pq} - (\frac{q\pi}{b})^2 + k^2_{mn}]\, A_{pq}\, e^{\mp \alpha_{pq} x} \cos \frac{q\pi y}{b} = 0 \tag{12}$$

This equation is true for all values of x and y within the region under consideration provided that

$$\alpha^2_{pq} = (\frac{q\pi}{b})^2 - k^2_{mn} \tag{13}$$

When boundary conditions (7) and (8) are applied to the assumed solutions (10) and (11), and the terms of the same y-dependence are set equal to zero, the result will be

$$A_{pq}\, e^{-\alpha_{pq} a} = C_{pq} \cos \beta_{pq} a \tag{14}$$

$$\alpha_{pq} A_{pq}\, e^{-\alpha_{pq} a} = \beta_{pq} C_{pq} \sin \beta_{pq} a \tag{15}$$

In order to have nontrivial solutions of the expansion coefficients A and C, Eqs. (14) and (15) yield the following conditions which must be satisfied:

$$\alpha_{pq} = \beta_{pq} \tan \beta_{pq} a \tag{16}$$

This is called the secular equation for the even TE modes.

When a similar procedure is carried out for region II by substituting Eq. (11) into Eq. (5) it can be verified that

$$\sum_{p,q} [k^2_{mn} h^2 - L^2_{pq}] \; C_{pq} \cos \beta_{pq} x \cos \frac{q\pi y}{b} = 0 \qquad (17)$$

where

$$L_{pq}^{\;2} = \beta_{pq}^{\;2} + (\frac{q\pi}{b})^2$$

Multiplying Eq. (17) by $(\sqrt{\epsilon_q \epsilon_s}/2ab) \; \cos \beta_{rs} x \cos \frac{s\pi y}{b}$, and integrating over the cross section of region II yields

$$\sum_{p,q} (k^2_{mn} H_{rspq} - L_{pq}^{\;2} F_{rspq} \delta_{sq}) \; C_{pq} = 0 \qquad (18a)$$

where $$\epsilon_q, \epsilon_s = \begin{cases} 1 & \text{if } q,s = 0 \\ 2 & \text{if } q,s \neq 0 \end{cases}$$

$$H_{rspq} = (\sqrt{\epsilon_q \epsilon_s}/_2 ab) \int_0^b \int_{-a}^{a} \cos \beta_{rs} x \cos \frac{s\pi y}{b} h^2(x,y) \cos \beta_{pq} x \cos \frac{q\pi y}{b} \, dx \, dy \qquad (18b)$$

$$F_{rspq} = {}^1/_{2a} \int_{-a}^{a} \cos \beta_{rs} x \cos \beta_{pq} x \, dx$$

$$\delta_{sq} = (\sqrt{\epsilon_q \epsilon_s}/_b) \int_0^b \cos \frac{s\pi y}{b} \cos \frac{q\pi y}{b} \, dy$$

The set of nontrivial solutions of the expansion coefficients C requires the determinant resulting from Eq. (18a) to vanish. Therefore

$$\det \left| k^2 H_{rspq} - L^2_{pq} \; F_{rspq} \; \delta_{sq} \right| = 0 \tag{19}$$

Each root of k^2 in Eq. (19) corresponds to a specific TE_{mn} mode.

The three equations (13), (16), and (19) provide a means of solving for the three unknowns α_{pq}, β_{pq}, and k_{mn}. Unfortunately exact solutions are not readily accessible, and it is imperative that approximate methods be utilized.

A first step in this solution is to limit the summations in Eqs. (10) and (11) to a finite number of terms such that the neglected higher order coefficients A_{pq} and C_{pq} are negligible. This is true if $|m - p|$ and $|n - q|$ are much larger than unity and the area of the cross-section of the groove is relatively small. This assumption makes Eq. (19) a finite determinant.

Let the zero-order approximation be investigated first. The characteristic value $(k^2_{mn})^{(o)}$ may be obtained by setting $\beta_{pq} = p\pi/a$ in Eq. (19). This case is then similar to the Rayleigh-Ritz method[4,5] for solution of the nonuniformly filled rectangular waveguide. The guide is constructed by adding two conducting walls at $x = \mp a$ to the nonuniformly filled parallel-plane guide.

With the knowledge of $(k^2_{mn})^{(o)}$, the zero-order values of α_{pq} and β_{pq} can be found from Eqs. (13) and (16). The zero-order values of α_{pq} and β_{pq} are then substituted into Eq. (19), from which a first-order approximation of k^2_{mn} is found. This procedure can be repeated until fairly good approximate values for k^2_{mn}, α_{pq}, and β_{pq} are obtained. The convergence is assured here since k^2_{mn} is smallest for $\beta_{pq} = p\pi/a$, and Eqs. (13) and (16) yield values too big for α_{pq} and β_{pq} which in turn, when substituted in Eq. (19), yield a larger value of k^2_{mn}. Larger values of k^2_{mn} produce smaller α_{pq} and β_{pq}. Furthermore, β_{pq} is not sensitive to the change in α_{pq}, as long as α_{pq} is not small.

Similar to the form of the even solution, the odd solution is expressed by:

$$\psi_o^{I} = \sum_{pq} A_{pq} \, e^{-\alpha_{pq} x} \cos \frac{q\pi y}{b} \tag{20}$$

$$\psi_o^{II} = \sum_{pq} C_{pq} \sin \beta_{pq} x \cos \frac{q\pi y}{b} \tag{21}$$

$$\psi_o^{III} = - \sum_{pq} A_{pq} \, e^{\pm \alpha_{pq} x} \qquad (22)$$

where the subscript "o" represents the odd solution. When similar procedures are followed, Eqs. (13) through (19) result, with the exception in Eq. (16) where tan $\beta_{pq} a$ would be replaced by $- \cot \beta_{pq} a$, and in Eqs. (18) and (19), the term $\cos \beta_{pq} x$ would be replaced by $\sin \beta_{pq} x$. The zero-order approximation is accomplished by letting $\beta_{pq} = \pi/2a\,(2p + 1)$.

b. <u>TM Modes:</u>

The wave function in Eq. (5) represents $E_z(x,y)$ for the case of TM modes. The boundary conditions of Eqs. (7) and (8) are valid here. However, the third condition should state that at $y = 0, b$, the wave function ψ is identically zero. The even solution of the equation is then assumed to be as follows:

$$\psi_e^{\substack{I \\ III}} = \sum_{pq} A_{pq} \, e^{\mp \alpha_{pq} x} \sin \frac{q\pi y}{b} \qquad (23)$$

and

$$\psi_e^{II} = \sum_{pq} C_{pq} \cos \beta_{pq} x \sin \frac{q\pi y}{b} \qquad (24)$$

Following the same procedure and applying the boundary conditions, Eqs. (13) through (19) result, with the exception of the function $\cos \frac{q\pi y}{b}$ which must be replaced by $\sin \frac{q\pi y}{b}$. The same argument applies to the odd solution of the wave equation.

4. CLASSIFICATION OF WAVE MODES IN GROOVE GUIDES

While the TEM mode propagates in parallel-plate waveguides, it will propagate in a groove guide, for the groove itself distorts the field pattern only slightly at the center region. However, the wave will suffer high attenuation which increases with frequency. There is no advantage, therefore, in using groove guides for the transmission line mode. The interesting feature of this unconventional guide is the transmission of the TE and TM modes.

Upon examination of Eq. (13), it can be seen that the values of α_{pq} may be real, imaginary, or zero. Wave modes will therefore be classified accordingly into three different classes.

(i) Propagating modes: Those modes have real values of α_{pq} which come from the fact that k_{mn} is less than $(q\,\pi/b)$ for all values of q. These modes will propagate in the longitudinal (z) direction and suffer exponential decay in the transverse direction.

The TE_{01}, TM_{11} and TM_{12} belong to this class because there is no contribution to the mode functions Eqs. (10), (11), (23) and (24) from terms with $q = 0$. (Note that for modes with odd n, no terms with even q contribute to the mode functions, and vice versa.) Also D_{0101} of TE_{01}, D_{1111} of TM_{11}, and D_{1212} of TM_{12} are greater than 1/2 where the quantity D_{rspq} is equal to H_{rspq} in Eq. (18) when β_{pq} and β_{rs} are replaced by $(p\,\pi/a)$ and $(r\,\pi/a)$ respectively. These ensure that k obtained from Eq. (19) is smaller than π/b for TE_{01} and TM_{11}, and smaller than $2\pi/b$ for TM_{12}.

(ii) Nonpropagating modes: They are the mode for which α_{pq} in Eq. (13) is imaginary, or k_{mn} is larger than $(q\,\pi/b)$ for some values of q. Imaginary values of α_{pq} change the nature of the mode function of Eq. (10) to represent propagation in the $\mp$ x-direction. The relative magnitudes of the coefficients A_{pq} remain unchanged for one mode. Therefore, the finite energy of a mode with imaginary α_{pq} attenuates rapidly by radiation. Wave modes belonging to this classification are $TE_{m,2n}$ where $m, n = 1, 2, 3, \ldots$, because α_{p0} is always imaginary.

(iii) Conditional propagation modes: If k_{mn} is equal to $(q\,\pi/b)$, the decay constant assumes its critical value of zero. The critical values of k_{mn} determined by Eq. (19), depend on the distance between the two parallel plates, and on the size of the grooves. These values of k are obtained from roots higher than those of the propagating modes. With $\alpha = 0$, Eq. (16) gives $\beta_{pq} = p\pi/a$ for even modes; similarly $\beta_{pq} = (2p+1)\pi/2a$ for odd modes. The modes $TE_{m+1,\ 2n+1}$ and $TM_{m+2,\ n+3}$ for $m, n = 0, 1, 2 \ldots$ are conditionally propagating modes for which the critical values of k_{mn} are:

$$(k_{mn})_c = \pi/b \text{ for } TE_{m+1,\ 2n+1} \text{ and } TM_{m+2,\ 2n+1} \text{ modes} \tag{25a}$$

$$(k_{mn})_c = 2\pi/b \text{ for } TM_{m+2,\ 2n} \text{ modes} \tag{25b}$$

From another point of view, the critical value of k_{mn} for TE mode is determined by setting the next higher order mode cut-off frequencies of a grooved rectangular waveguide, which is formed by placing two additional conducting plates at $x = \mp\ a$ of the groove guide, equal to the lowest cut-off frequency of a parallel-plane waveguide without a groove. A similar procedure will determine the conditions for transmission of TM modes. Hence, for a given groove-guide, the transmission condition can be found. However, for given b and the shape of the groove, it is not in general, possible to determine the size of the groove by Eq. (19) except by trial and error method. A rectangular groove guide can be determined by the transverse resonance method.[2]

5. DECAY CONSTANT

The TE_{01} mode is the dominant mode, and will be discussed in more detail; it is the only mode to be considered in the rest of this paper. Other modes can be analyzed in a similar manner.

The decay constants α_{pq} given by Eq. (13) are independent of the operating frequency. The constants depend, however, on the size and shape of the groove, and on the distance between the two plates of the guide.

For the TE_{01} mode, α_{pq} is much smaller than all other decay constants as shown by Eq. (13), and A_{01} is much larger than all other expansion coefficients. Therefore, at distances away from the center, Eq. (10) may be approximated as

$$\psi^{\mathrm{I}}_{\mathrm{III}} \approx e^{\mp \alpha_{p1} x} \cos \pi y/b \sum_p A_{p1}$$

The existence of real values of the decay constant for the groove guide allows making the wall width finite and practical. In contrast, the parallel-plate guide has no decay constant in the transverse direction and consequently radiation losses are quite significant for walls of inite width.

6. ATTENUATION CONSTANT

The attenuation due to the finite conductivity of the waveguide walls can be found by conventional methods. The attenuation constant is defined as the ratio of the power dissipated in the walls to twice the power density flow between the walls, assuming lossless dielectric filling the waveguide. The field distributions are given in Eqs. (10) and (11). After some manipulation, the attenuation constant for the groove guide can be shown as follows:

$$\text{Att.} = (\text{Att.})_p \left(\frac{f_c}{f_{cp}}\right)^4 \left[1-\left(\frac{f_{cp}}{f}\right)^2\right]^{1/2} \cdot \left[1-\left(\frac{f_c}{f}\right)^2\right]^{-1/2} \cdot G$$

where $(\text{Att.})_p$ = Attenuation constant of an air-filled parallel plane waveguide

f_{cp} = Cut-off frequency of the parallel-plane waveguide.

f_c = Cut-off frequency of the groove guide.

f = Operating frequency

The G factor is a length expression, approximately equal to unity, and depends slightly on frequency. To show the order of magnitude of G, it can be approximated by

$$G \approx 1 + \frac{k_3^2 \ \beta_{01}^2}{k_{01}^4} \left(\frac{2\beta_{01}a - \sin 2\beta_{01}a}{2\beta_{01}a + \sin 2\beta_{01}a}\right)$$

for TE_{01} mode, where all higher order terms are neglected.

The last term on the right hand side is, in general, much less than unity and therefore may be neglected.

Since the decay constants are real for the propagating modes, f_c is smaller than f_{cp}. The attenuation constant of the groove guide is, therefore, less than that of the parallel-plane waveguide at all frequencies above cutoff. This is one of the salient features of the groove guide.

7. EXPERIMENTAL RESULTS

To verify the preceding theory of the groove guide, a structure has been designed as shown in Fig. 3. The rectangular groove depth is 0.1575 inch and its width is 0.3 inch. The guide width is 0.9 inch, the same as that of an X-band rectangular guide.

The expression of the scale factor h has been derived by Tischer[3],

$$h^2 = \left[\frac{(r_2 - \cos\phi \cosh\theta)^2 + (\sin\phi \sinh\theta)^2}{(r_1 - \cos\phi \cosh\theta)^2 \quad (\sin\phi \ \sinh\theta)^2} \right]^{1/2}$$

where $\phi = 2\pi y/b$ and $\theta = 2\pi x/b$. The scalar quantities r_1 and r_2 are determined from Fig. 4 of Ref. 3, if the size of the groove is known. For the groove in this example $r_1 = 1.0291$ and $r_2 = 1.2748$. The quantities H_{rspq} are calculated by a digital computer. The integral of the region about the singularity $y = 0$ and $\theta = \cosh^{-1} r_1$ is evaluated by the open type integration method.[6] The second-order approximation of k^2_{01} is calculated by the method discussed in Sec. 3 and found to be

$$(k_{01}\, b)^2 = 0.89\ \pi^2$$

The decay factor $\alpha_{p1} = 0.456$ neper/cm and it is independent of frequency.

A groove guide was constructed out of aluminum with length of one meter and width of 15 cm. The ends of the guide were shorted by large plates of the same material, thus forming a groove guide cavity. The energy was fed to the cavity through a small hole located on one of the end plates between the grooves. The electromagnetic wave was launched by an X-band source set-up.

The groove guide wavelength was measured by introducing a probe moving along the open side of the groove guide cavity. The experimental values agree with the theoretical calculation as shown in Fig. 4. The cut-off frequency is 6.15 GC compared with 6.56 GC for parallel-plane waveguide of the same dimension.

The field distribution in the transverse direction was measured by Slater's perturbation method.[7] The shift of the resonant frequency of the cavity is proportional to the square of field strengths:

$$\frac{\Delta f}{f_o} = K_1 |E|^2 + K_2 |H|^2$$

where f_o is the resonant frequency, Δf is the deviation in frequency due to perturbation, and K_1 and K_2 are constants which depend on the geometry of the perturbing object. It can be seen that the ratio of the magnitudes of the fields squared at two different positions (x_1 and x_2) as

$$\frac{\Delta f_1}{\Delta f_2} = \exp \left[2 \alpha (x_2 - x_1) \right]$$

where α is the decay constant. Experimentally, a tiny metal sphere has been placed at different locations in the transverse direction of the cavity and parallel to its wall. The relative field strength squared was measured and plotted as shown in Fig. 5 at two different frequencies. The results agree with the theoretical curve which is calculated for $\alpha = 0.456$ neper/cm, and show that the decay constant is independent of frequency. There is, however, a discrepancy near the two edges of the guide, which is due to the finite width of the conducting plates. The field near the edges is approximately 0.1 of its peak value at the center of the groove for this waveguide.

The attenuation measurements were done by using cavity resonant methods. Barlow and Cullen[8] showed that for long cavities and neglecting the losses due to shorting plates

$$\text{Att.} = \frac{\pi}{Q} \frac{\lambda_g}{\lambda_o^2}$$

where λ_g is the guide wavelength, and λ_o is the free-space wavelength. The large difference between the experimental and the theoretical values of the attenuation constant (see Fig. 6) is due to the reduction of the cavity quality factor Q by the radiation from the open sides. This reduction amounts to about half the theoretical value for the present experimental configuration. If the cavity walls were wider, the discrepancy between the experimental and the theoretical values are expected to be reduced accordingly.

8. CONCLUSION

The boundary value problem of a groove guide has been solved by approximate techniques. The cut-off frequency, field distribution, and the attenuation constant were calculated. All the theoretical results were verified experimentally.

The outstanding features of the groove guide are the attenuation, transverse decay constant, and mode propagation. The attenuation is small and decreases with frequency. The transverse decay constant permits the parallel walls to be finite in width, without significant radiation losses. Under certain geometrical conditions, the propagation of TE modes is limited to the dominant mode only. These characteristics make the groove guide a wide-band waveguide, and practicable for higher frequency propagation.

REFERENCES

[1] J. M. Ruddy, "The Groove Guide," Memorandum No. 89, July 3, 1963, Polytechnic Institute of Brooklyn.

[2] Tsuneo Nakahara and Noritaka Kurauchi, "Transmission Modes in the Groove Guide," International Conference on Microwaves, Circuit Theory and Information Theory, Sept. 1964, (The Institute of Electrical Communication Engineers of Japan.)

[3] F. J. Tischer, "The Groove Guide, A Low-Loss Waveguide for Millimeter Waves," IEEE Trans. on Microwave Theory and Techniques, Vol. MTT-11, pp. 291-296, Sept. 1963.

[4] F. J. Tischer and H. Y. Yee, "Waveguides With Arbitrary Cross-Section Considered by Conformal Mapping," to be published.

[5] R. E. Collin, "Field Theory of Guided Wave," McGraw-Hill Book Company, Inc., New York, Chapt. 6, (1960).

[6] W. E. Milne, "Numerical Calculus," Princeton University Press, p. 126, (1949).

[7] E. L. Ginzton, "Microwave Measurements," McGraw-Hill Book Co., New York, Chapter 10, (1957).

[8] H. M. Barlow and A. L. Cullen, "Microwave Measurements," Constable and Co. Ltd., London, Chapter 3, (1950).

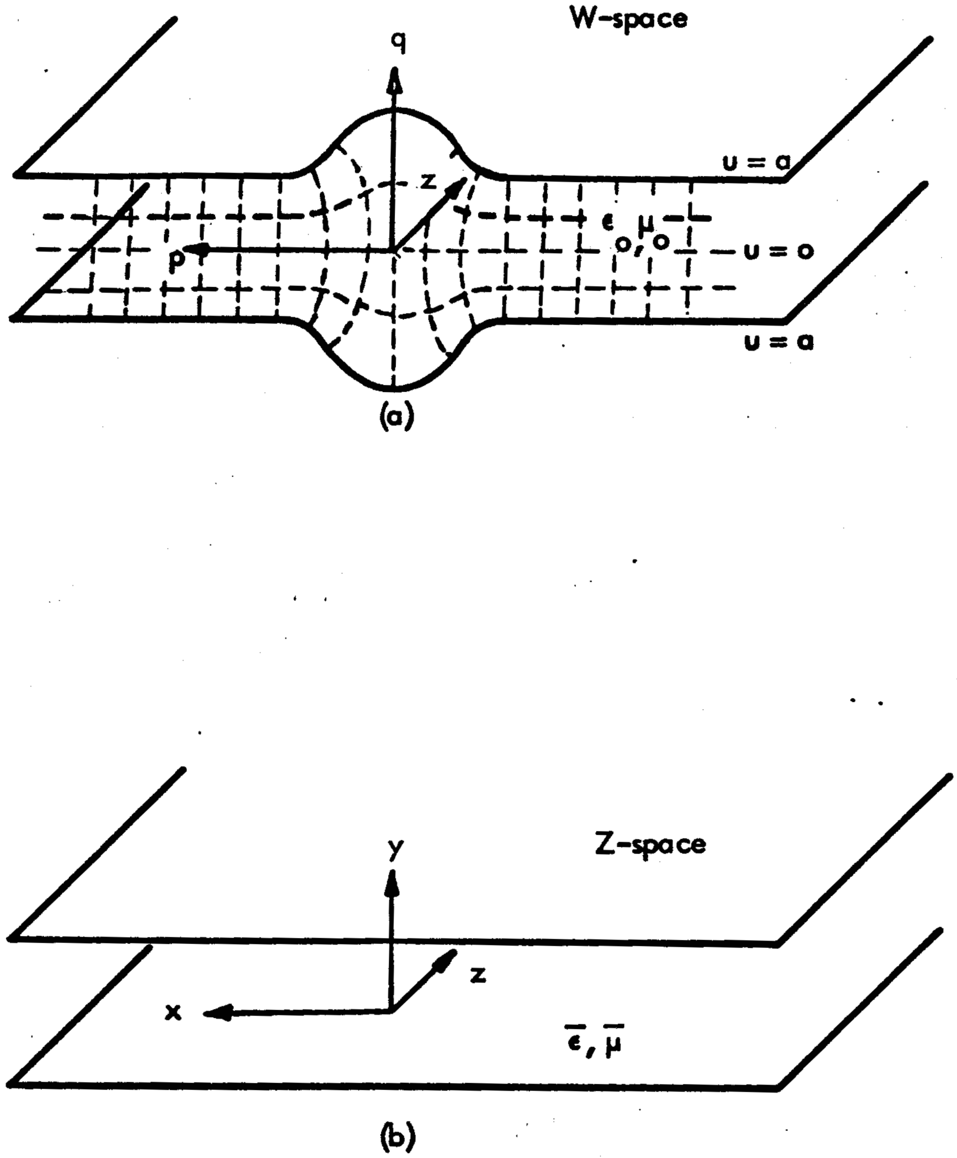

Fig. 1 - Conformal transformation of the groove guide.

(a) The groove guide in the W-space

(b) The equivalent parallel-plane guide in the Z-space

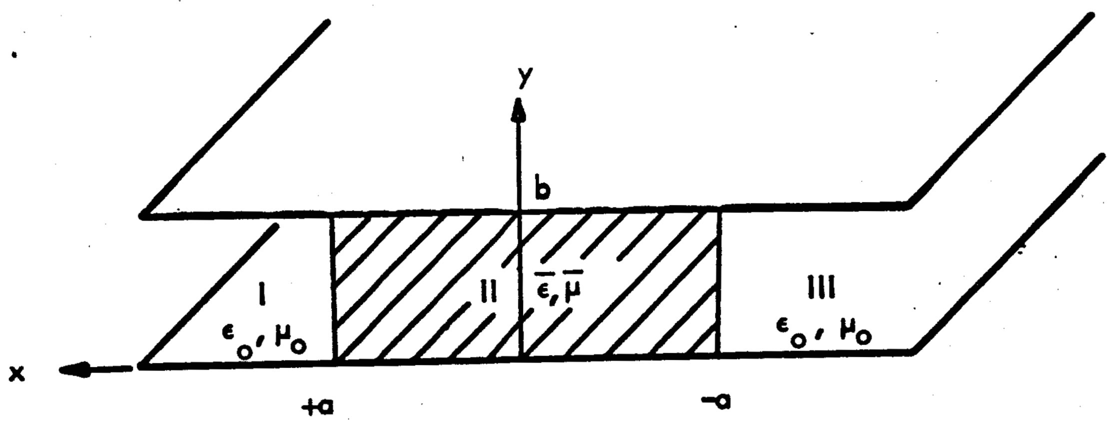

Fig. 2 - Approximation of the equivalent parallel-plane waveguide.

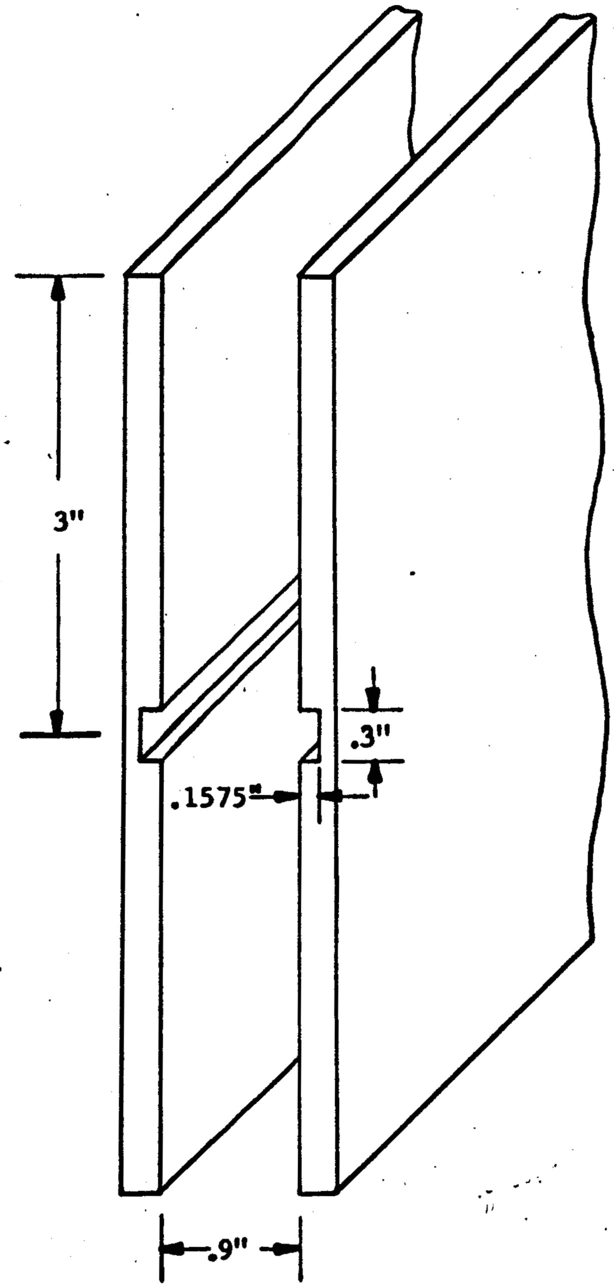

Fig. 3 - Groove guide cross sectional view.

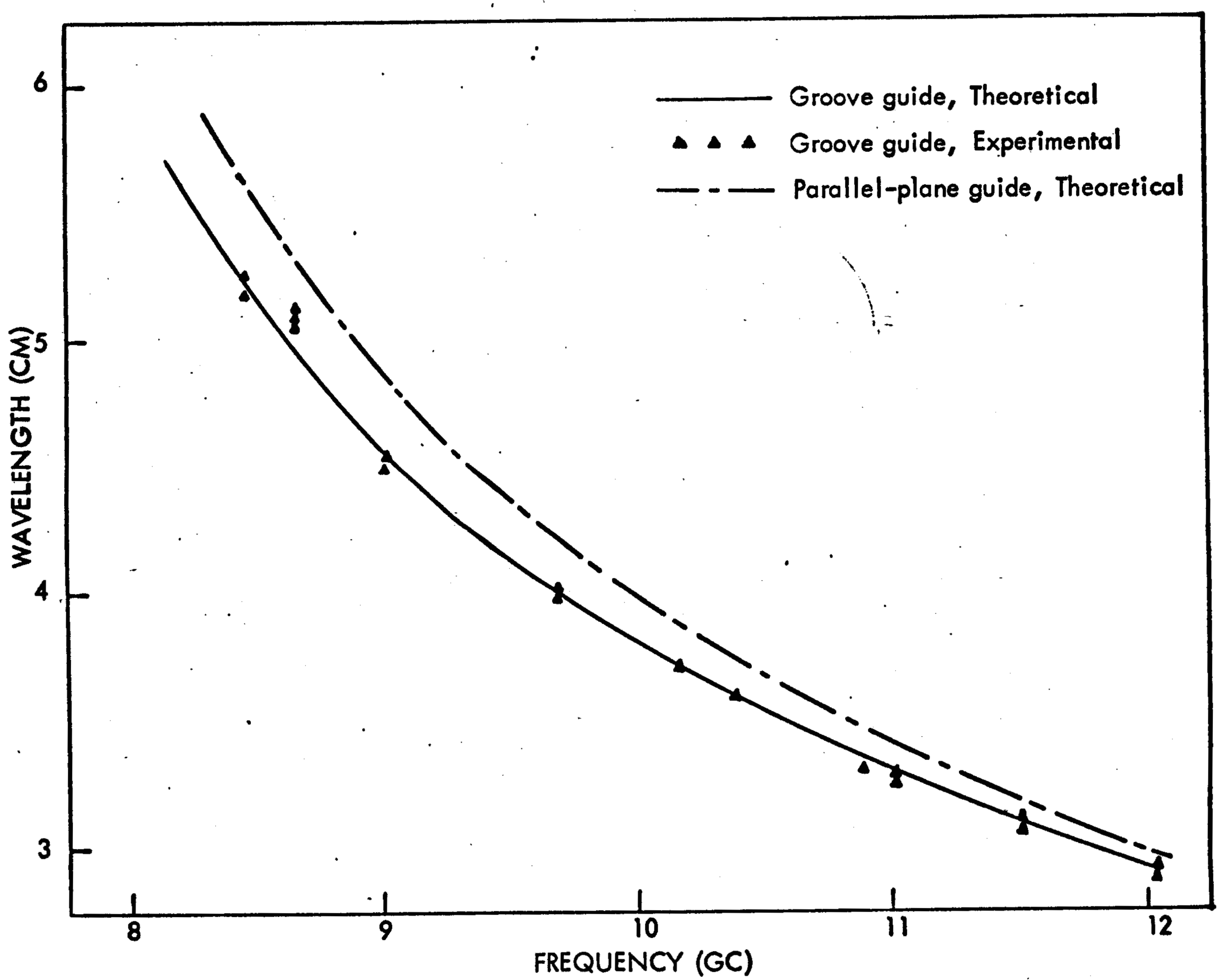

Fig. 4 - Wavelength vs. frequency curves for groove and parallel-plane waveguides.

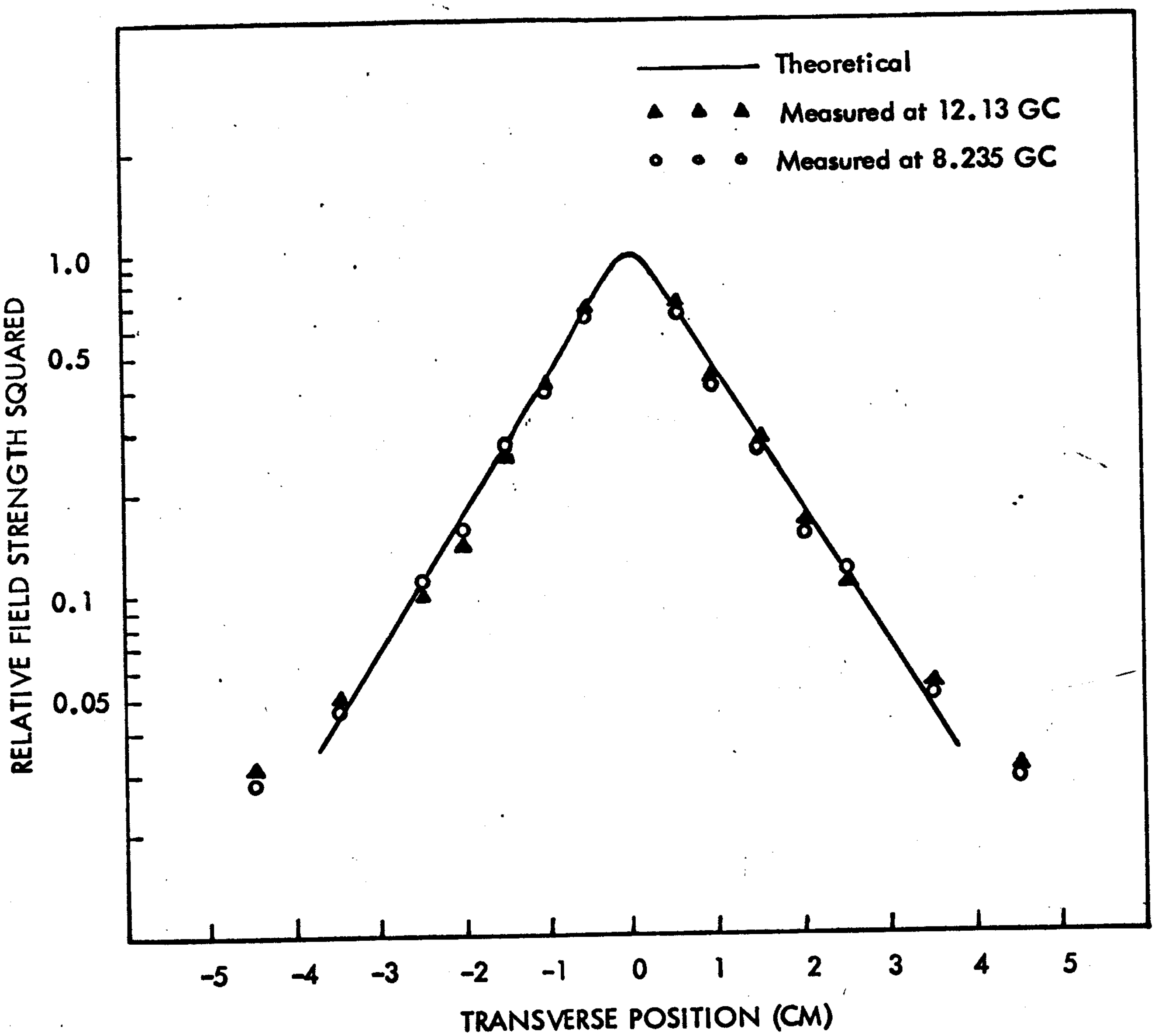

Fig. 5 - The distribution of the field strength squared as a function of the transverse position in the groove guide.

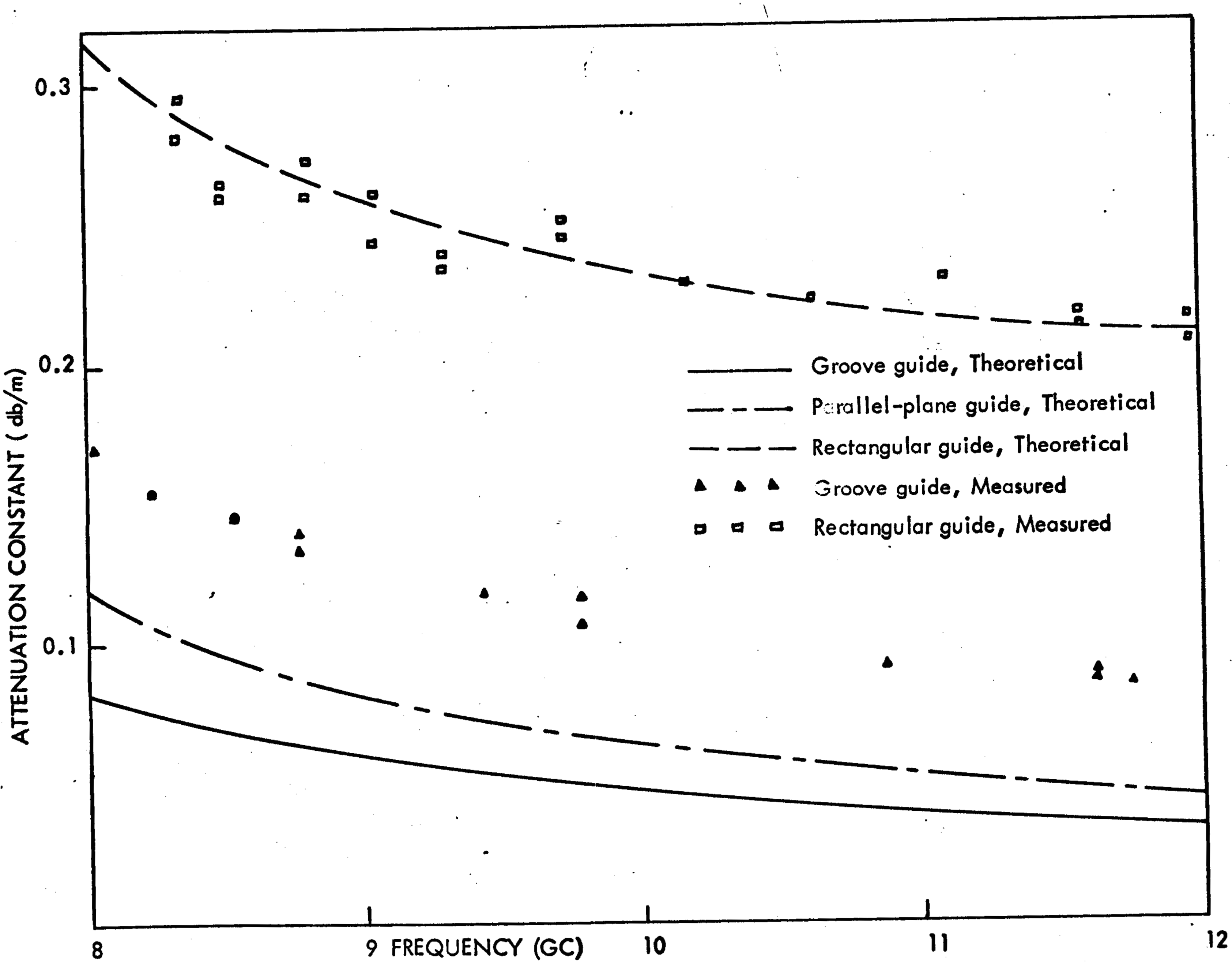

Fig. 6 - Attenuation vs. frequency curves for groove, parallel-plane, and rectangular waveguides.